Proc. Natl. Acad. Sci. USA
Vol. 95, pp. 5484–5489, May 1998
Biochemistry

Genetic, biochemical, and crystallographic characterization of Fhit–substrate complexes as the active signaling form of Fhit

HELEN C. PACE*, PRESTON N. GARRISON†, ANGELA K. ROBINSON†, LARRY D. BARNES†, ALEXANDRA DRAGANESCU*, ANGELIKA RÖSLER‡, G. MICHAEL BLACKBURN‡, ZURAB SIPRASHVILI*, CARLO M. CROCE*, KAY HUEBNER*, AND CHARLES BRENNER*§

*Kimmel Cancer Institute, Thomas Jefferson University, Philadelphia, PA 19107; †Department of Biochemistry, University of Texas Health Science Center, San Antonio, TX 78284; and ‡Department of Chemistry, Krebs Institute, University of Sheffield, Sheffield, S3 7HF England

Communicated by Sidney Weinhouse, Jefferson Medical College, Philadelphia, PA, March 2, 1998 (received for review December 1, 1997)

ABSTRACT **Alterations in the *FHIT* gene at 3p14.2 occur as early and frequent events in the development of several common human cancers. The ability of human Fhit-negative cells to form tumors in nude mice is suppressed by stable reexpression of Fhit protein. Fhit protein is a diadenosine P^1,P^3-triphosphate (ApppA) hydrolase whose fungal and animal homologs form a branch of the histidine triad (HIT) superfamily of nucleotide-binding proteins. Because the His-96 → Asn substitution of Fhit, which retards ApppA hydrolase activity by seven orders of magnitude, did not block tumor-suppressor activity *in vivo*, we determined whether this mutation affected ApppA binding or particular steps in the ApppA catalytic cycle. Evidence is presented that His-96 → Asn protein binds ApppA well and forms an enzyme-AMP intermediate extremely poorly, suggesting that Fhit–substrate complexes are the likely signaling form of the enzyme. The cocrystal structure of Fhit bound to Ado-p-CH_2-p-p_s-Ado (IB2), a nonhydrolyzable ApppA analog, was refined to 3.1 Å, and the structure of His-96 → Asn Fhit with IB2 was refined to 2.6 Å, revealing that two ApppA molecules bind per Fhit dimer; identifying two additional adenosine-binding sites on the dimer surface; and illustrating that His-98 is positioned to donate a hydrogen bond to the scissile bridging oxygen of ApppA substrates. The form of Fhit bound to two ApppA substrates would present to the cell a dramatically phosphorylated surface, prominently displaying six phosphate groups and two adenosine moieties in place of a deep cavity lined with histidines, arginines, and glutamines.**

The signaling states of many proteins depend on their association with a wide variety of purine nucleotides such as GTP, cAMP, cADP-ribose, and 7-methyl-GTP. Recently, we discovered that HIT proteins, dimeric proteins named for the HIT motif, His-ϕ-His-ϕ-His-ϕ-ϕ (ϕ is a hydrophobic amino acid), are structurally related to galactose-1-phosphate uridylyltransferase and contain two identical purine mononucleotide-binding sites per dimer (1). Proteins of the HIT superfamily fall into branches named for their mammalian prototypes, Hint and Fhit. Hint homologs are found in all forms of life, whereas Fhit homologs appear to be confined to animals and fungi. Fhit protein is of interest because the human *FHIT* gene (2) is a hot spot for early inactivation in carcinogen-exposed tissues (3) and in the development of several common cancers (4–10). *FHIT* encodes an enzyme with diadenosine P^1,P^3-triphosphate (ApppA) hydrolase activity *in vitro* (11). However, the cellular mechanism of Fhit activity, and the relationships between Fhit activity, the cellular pathways of Fhit, and cancer are not yet understood.

Because Fhit is encoded at the chromosome 3 fragile site, FRA3B (12), it had been suggested that cancer-associated deletions in the *FHIT* gene represent a "bystander effect" in which carcinogenesis was initiated by other unrelated genetic changes and that *FHIT* deletions resulted from genomic instability within already established tumors (13). However, if this were the case, reintroduction of *FHIT* cDNAs into tumors with *FHIT* deletions would not be expected to be consequential. On the contrary, stable reexpression of Fhit protein in gastric, lung, and kidney cancer cells with homozygous *FHIT* deletions suppressed the ability of those cells to form tumors in nude mice (14). It is important to emphasize that whereas *FHIT* passed this test as a tumor-suppressor gene, there are at least two scenarios in which genes with importance in carcinogenesis might fail this test. First, if loss of function of a gene were to create a mutator phenotype that led to further genetic lesions, reintroduction of that gene into tumor-derived cell lines might not reverse their tumor-forming ability. Second, in complex genetic backgrounds, it might be difficult to measure the effect of reintroduction of a single tumor-suppressor gene. Thus, the ability of *FHIT* reexpression to reduce tumor formation in animals is a strong, positive result demonstrating antagonism of Fhit protein to transformed cell growth or survival (14).

Given the activity of Fhit as a tumor suppressor, we considered three mutually exclusive cellular mechanisms for tumor-suppressing activity with respect to the biochemical activity of Fhit as an ApppA hydrolase. First, the tumor-suppressing function of Fhit might be to *catabolize* ApppA or related substrates. Second, the tumor-suppressing function of Fhit might be *signaling by Fhit-bound forms* of these compounds. Third, Fhit might have a *nucleotide-independent* role as a tumor suppressor. The differences between these three models are highly significant.

If, according to the first mechanism, the activity of Fhit as a tumor suppressor were to depend on clearing the cell of ApppA or related substrates, then mutations that block the ability of the enzyme to cleave substrates would be expected to result in loss of tumor-suppressor activity. Furthermore, a catabolic mechanism would suggest that Fhit substrates have a tumor-promoting activity mediated by a cellular factor that is present in the absence of Fhit protein.

If, according to the second mechanism, Fhit were to function by signaling the presence of Fhit substrates, then mutations

Abbreviations: ApppA, diadenosine P^1,P^3-triphosphate; IB2, Ado-p-CH_2-p-p_s-Ado; HIT, histidine triad; CHESS, Cornell High Energy Synchrotron Source.

Data deposition: The atomic coordinates and structure factors have been deposited in the Protein Data Bank, Biology Department, Brookhaven National Laboratory, Upton, NY 11973 (references: wild-type Fhit–IB2, 1FHI; His96Asn Fhit–IB2, 2FHI).

§To whom reprint requests should be addressed at: Kimmel Cancer Institute, Thomas Jefferson University, 233 S. 10th Street, Rm. 826, Philadelphia, PA 19107. e-mail: brenner@dada.jci.tju.edu.

The publication costs of this article were defrayed in part by page charge payment. This article must therefore be hereby marked "*advertisement*" in accordance with 18 U.S.C. §1734 solely to indicate this fact.

that block the ability of the enzyme to bind substrates would be expected to result in loss of tumor-suppressor activity. There are two biochemically distinct ways in which Fhit might signal to the cell that high levels of Fhit substrates have been made. In the simplest case, the *enzyme–substrate* complex might activate an anti-proliferative or pro-apoptotic effector in a manner reminiscent of signaling by the GTP-bound form of G proteins. Alternatively, a slow step in the cleavage reaction might exist that allowed an *enzyme-intermediate* such as Fhit-AMP to signal through an anti-proliferative or pro-apoptotic effector. In these models, cleavage of Fhit substrates or hydrolysis of Fhit-intermediates would be expected to terminate signaling.

Finally, according to the third mechanism, if the function of Fhit as a tumor suppressor were unrelated to nucleotide substrates, then it might be possible to reduce the ability of Fhit to interact with substrates without affecting tumor-suppressor activity.

The ability to evaluate these three cellular mechanisms depends on the ability to generate and to assay discrete biochemical phenotypes with respect to nucleotide interactions and to measure resulting *FHIT* alleles in tumor-suppressor assays. The crystal structure of rabbit Hint bound to 8-Br-AMP and GMP identified 14 conserved residues in HIT proteins that make intimate contact with the purine bases, the ribose, or the α-phosphate (1). Mutations that disturb interactions with the α-phosphate would be expected to reduce cleavage of HIT protein substrates without affecting the ability of those substrates to bind. On the other hand, mutations that occlude the base-binding site would be expected to hinder nucleotide binding.

His-112 of Hint, along with Asn-99 and His-114, corresponding to His-96, Gln-83, and His-98 of Fhit, were identified as the key residues surrounding the α-phosphate in nucleotide-bound forms of Hint that were predicted to affect cleavage but not binding of specific Fhit substrates (1). Mutation of His-96 to Asn was shown to reduce ApppA hydrolase activity by more than three orders of magnitude in a nonpurified system (11). Strikingly, this mutation did not reduce the tumor-suppressor activity of replaced *FHIT* cDNAs in the nude mouse assay (14), suggesting that the tumor-suppressing activity of Fhit is not catabolic. To determine whether phenotypic analysis of this allele provided evidence for a nucleotide-independent mechanism of Fhit function or a cellular mechanism that depends on formation of an enzyme–substrate or an enzyme–intermediate complex, the His-96 → Asn mutant form of Fhit protein (hereafter called His96Asn Fhit) was purified and characterized biochemically. Data are presented that establish only a 4-fold defect in K_m of the His96Asn mutant enzyme for ApppA, and a $>10^6$-fold defect in k_{cat}, most of which is evident in the first measurable chemical step of the reaction. These data are consistent with the idea that the biologically active form of Fhit is the enzyme–substrate complex.

Three crystalline forms of Fhit have been prepared to model the enzyme–substrate complex: wild-type enzyme bound to Ado-p-CH_2-p-p_s-Ado [IB2; a nonhydrolyzable ApppA analog (15)], His96Asn protein bound to ApppA (15), and His96Asn protein bound to IB2. Here we use coordinates of unliganded Fhit protein (16) to solve the structures of wild-type and His96Asn Fhit proteins bound to IB2 (17), revealing that the Fhit dimer binds two ApppA substrates, displaying the third and fourth adenosines and six surface phosphate groups as a potential molecular signal to cytosolic effectors. Though the third potential mechanism of Fhit function, that tumor-suppressor function is unrelated to nucleotide interactions, is not eliminated by this study, residues are identified in the cocrystal structures whose substitution would be expected to hinder the ability of Fhit to bind substrates without denaturing the protein.

MATERIALS AND METHODS

Soluble and Crystalline Fhit Proteins. Purification of wild-type and His96Asn Fhit proteins and their crystallization in space group *P*6(1)22 have been described (15). Cell lengths for the His96Asn–IB2 complex refined to $\alpha = \beta = 50.46$ Å, $\gamma = 268.95$ Å, and, as with other Fhit crystals (15, 16, 18), required synchrotron radiation for data collection. Synthesis of IB2 has been described (17). Cryogenic data for the complex of wild-type Fhit with IB2 were collected at beamline F1 of the Cornell High Energy Synchrotron Source (CHESS) as described (15). Cryogenic data for the complex of His96Asn Fhit with IB2 were collected at CHESS F1 with an ADSC Quantum-4 detector located 200 mm from the crystal in 8-s, 0.25° oscillations. Reflections (36,336 observations from 22-Å to 2.0-Å resolution) were indexed and integrated with MOSFLM and scaled with SCALA (19) to produce 12,563 unique intensities (87.5% complete, $R_{sym} = 9.7\%$).

Steady-State Assays of Fhit Proteins. Reactions (100 μl) in 50 mM Na Hepes, pH 6.8/0.5 mM $MnCl_2$/2% glycerol were performed at 37°C as a function of concentration of [^{3}H]ApppA and were quantitated by counting radioactivity in peaks of [^{3}H]AMP and [^{3}H]ADP products after separation on a boronate-derivatized resin (20). For assays of wild-type enzyme, <1 ng of wild-type enzyme was used per 10-min reaction, and these reactions included 20 μg of bovine serum albumin. For assays of His96Asn enzyme, 30–40 μg of Fhit was used in 2- to 3-h incubations. For reasons that were not apparent, the concentration dependence of His96Asn Fhit activity was observed to be slightly cooperative (Hill coefficient = 1.3). Data for this mutant were fit to the Michaelis–Menten equation with substrate concentration raised to the power of 1.3. Results, summarized in Table 2, are means ± SD for three wild-type and five His96Asn experiments.

Single-Turnover Assays of Fhit Proteins. Reactions, in 10 μl of 50 mM Na Hepes, pH 6.8/0.5 mM $MnCl_2$ containing 5 nmol of ApppA, were initiated by addition of 5 nmol (protein concentration refers to monomers) of homogeneous wild-type or His96Asn Fhit protein. At indicated times of incubation at 37°C, 1-μl samples were spotted on aluminum-backed silica TLC plates with fluorescent indicator and developed with standard methods (11). Nucleotides were visualized by UV-shadowing.

Crystallographic Refinement. Unliganded, isomorphous Fhit protein coordinates (1FIT) kindly provided by Christopher D. Lima (16) had an initial *R* factor for the wild-type Fhit-IB2 data set of 40.6%. Coordinates were subjected to rigid-body, positional, and B-factor refinement and simulated annealing in X-PLOR version 3.851, guided by reduction of the free *R* factor of test-set reflections (21). Reflections omitted from refinement ($F/\sigma < 3.5$ for the wild-type complex, $F/\sigma < 3$ for the His96Asn complex) were not excluded from difference electron density maps such as shown in Fig. 3. Simulated annealing omit maps were calculated in five-residue sections of

Table 1. Refinement statistics of Fhit–IB2 models

Complex with IB2	Residues	Water molecules	Resolution, Å	Reflections		*R* factor		rms deviations from ideality	
				No.	% (% last shell)	Working	Free	Bond lengths, Å	Bond angles, °
Wild type	2–106, 128–147	3	8–3.1	2,660	64.6 (36.3)	0.240	0.312	0.010	1.5
His96Asn	2–106, 129–147	32	6–2.6	5,718	84.0 (83.4)	0.241	0.278	0.015	1.8

the protein model to rebuild the structures in O version 6.1.1 (22) with (F_{obs} − F_{calc}) difference electron density. Water molecules with good geometry and substantial difference density were added. When the working *R* factors fell to below 30%, ($2F_{obs}$ − F_{calc}) and (F_{obs} − F_{calc}) electron density indicated the presence and the orientation of one molecule of IB2, the nonhydrolyzable substrate analog, per Fhit monomer in the asymmetric unit of each complex. IB2 (Ado-p-CH_2-p-p_s-Ado) is an ApppA analog with a methylene substitution for the P^1–P^2 bridging oxygen and a sulfur substitution for a P^3 phosphate oxygen (17). The compound has two stereoisomers about the thiophosphate center and could potentially bind with P^1 or P^3 nearest His-96. In the complex with wild-type Fhit, the largest peak of difference electron density, near Leu-100, was stereospecifically assigned to the sulfur of IB2 in the *S* configuration, placing the P^1 phosphate near His-96 and the P^1–P^2 methylene near His-98. In the complex with His96Asn Fhit, the largest peak of difference density, modeled as the P^3 thiophosphate group in the *R* conformation, was present nearest Asn-96. Though it is possible to "refine" the models to working *R* factors below 20%, the structural models presented herein have good geometry and are at apparent free *R*-factor minima, values of which are likely limited by disorder that prevents modeling of residues 107–128. Refinement statistics are summarized in Table 1.

Molecular Calculations and Graphics. Figs. 2, 3, 4, and 6 were prepared with MOLSCRIPT version 1.4 (23), Povscript (http://www.rose.brandeis.edu/users/peisach/povscript/info.html), and POV Ray Tracer version 3.01 (http://www.povray.org). The surface electrostatic calculation for Fig. 5 was prepared with DELPHI (24) at 0.15 M ionic strength.

RESULTS

His96Asn Fhit Protein Binds ApppA. As summarized in Table 2, prolonged incubation of His96Asn Fhit protein revealed specific, protein- and time-dependent, ApppA hydrolytic activity that is saturable with respect to ApppA substrate in the low micromolar range. Though the catalytic defect of His96Asn, judged by reduction in k_{cat}/K_m, exceeds seven orders of magnitude, the K_m of the mutant enzyme for ApppA is only 4 times that of wild type, whereas k_{cat} lags that of the wild type by more than six orders of magnitude.

His96Asn Fhit Protein Is Defective in the First Measurable Chemical Step of ApppA Hydrolysis. Kinetics of ApppA cleavage by wild-type Fhit protein suggested that the enzyme attacks ApppA rapidly, releasing ADP and forming a covalent enzyme-AMP intermediate. Hydrolysis of the enzyme-AMP intermediate appeared to be the rate-limiting step in the reaction (18). If the huge defect in steady-state ApppA hydrolase activity by His96Asn Fhit were because of formation of a putative enzyme-AMP intermediate at a normal rate and a specific defect in hydrolysis or release of AMP, then the role of Fhit as a tumor suppressor might be mediated by the enzyme-AMP intermediate. Fhit assays were performed with sufficient enzyme to visualize the products of one molar equivalent of ApppA by UV-shadowing on TLC plates. As the calculated $t_{1/2}$ of the wild-type enzyme for the complete (ApppA + H_2O → AMP + ADP) reaction is 10 ms, it was not surprising that wild-type reaction was complete within the first (15 s) time point (Fig. 1). If His96Asn Fhit protein were defective only in the second step of the reaction, one would expect one equivalent of ADP to be released with wild-type

Table 2. Kinetic parameters of Fhit

Enzyme	k_{cat}, monomer^{-1}·s^{-1}	K_m, μM	k_{cat}/K_m, s^{-1}·M^{-1}
Wild type	$(7.3 \pm 4.3) \times 10^1$	1.9 ± 0.2	$(3.8 \pm 2.2) \times 10^7$
His96Asn	$(1.8 \pm 0.4) \times 10^{-5}$	7.5 ± 2.3	2.5 ± 0.6

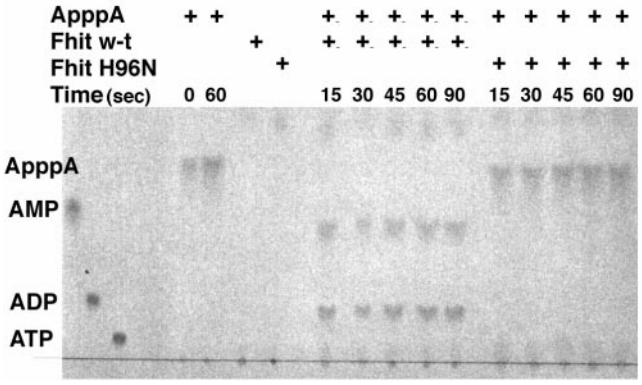

FIG. 1. Single-turnover assay of wild-type and mutant Fhit proteins. Purified wild-type (w-t) and His96Asn (H96N) Fhit proteins (5 nmol monomers) were incubated at 37°C with 5 nmol ApppA in 10 μl. At indicated times, 1-μl samples were spotted on TLC plates along with appropriate standards. Consumption of ApppA and release of ADP with normal kinetics by His96Asn would have indicated a specific defect in deadenylation. Extremely slow production of ADP and AMP indicates a defect in the first (and possibly all) chemical steps.

kinetics. Fig. 1 shows that mutant enzyme is retarded in the first measurable chemical step in the reaction, releasing no ADP at a 90-s time point. Longer incubations (not shown) demonstrate that AMP and ADP are released concomitantly with a $t_{1/2}$ of 3–6 h, suggesting that, for this mutant, formation of a putative enzyme-AMP intermediate is rate-limiting and is greatly retarded by the amino acid substitution. Because the His96Asn mutant form of Fhit, active in tumor-suppressor assays (14), binds ApppA well but is severely defective in ApppA hydrolytic activity and the ability to form a putative Fhit-AMP intermediate, we reasoned that the enzyme–substrate complex is the active, signaling form of Fhit.

Wild-Type and Mutant Fhit Protein Dimers Bind Two ApppA Analogs with HIT-Specific and Fhit-Specific Amino Acids. We previously observed that Hint protein structures are not significantly changed by binding mononucleosides or mononucleotides (1). The Fhit protein structure in Fhit–IB2 crystals is folded as is Fhit in apo, adenosine-bound, and adenosine [α,β-methylene]diphosphate-bound forms, and in a form crystallized with adenosine plus tungstate (16, 18). Like other HIT proteins, Fhit appears to be constitutively dimeric.

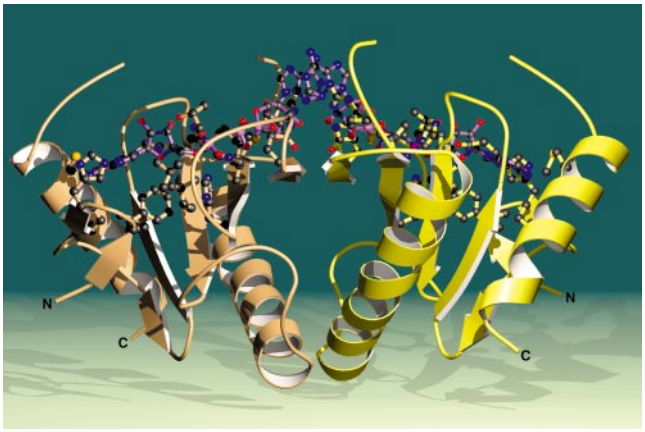

FIG. 2. Architecture of Fhit–IB2 complexes. Side view of the wild-type Fhit dimer with two bound IB2 molecules. Monomers of Fhit are yellow and copper; IB2 molecules are purple. All nonhydrogen atoms are shown for IB2 and for amino acid side chains surrounding the dinucleotides (Phe-5, His-8, Ile-10, Leu-25, Asn-27, Val-31, His-35, Leu-37, Thr-79, Gln-83, Thr-91, Val-92, His-96, His-98, Leu-100, Arg-102, and Met-135). Atoms are colored as follows: carbon, black; nitrogen, blue; oxygen, red; phosphorus, magenta; sulfur, orange.

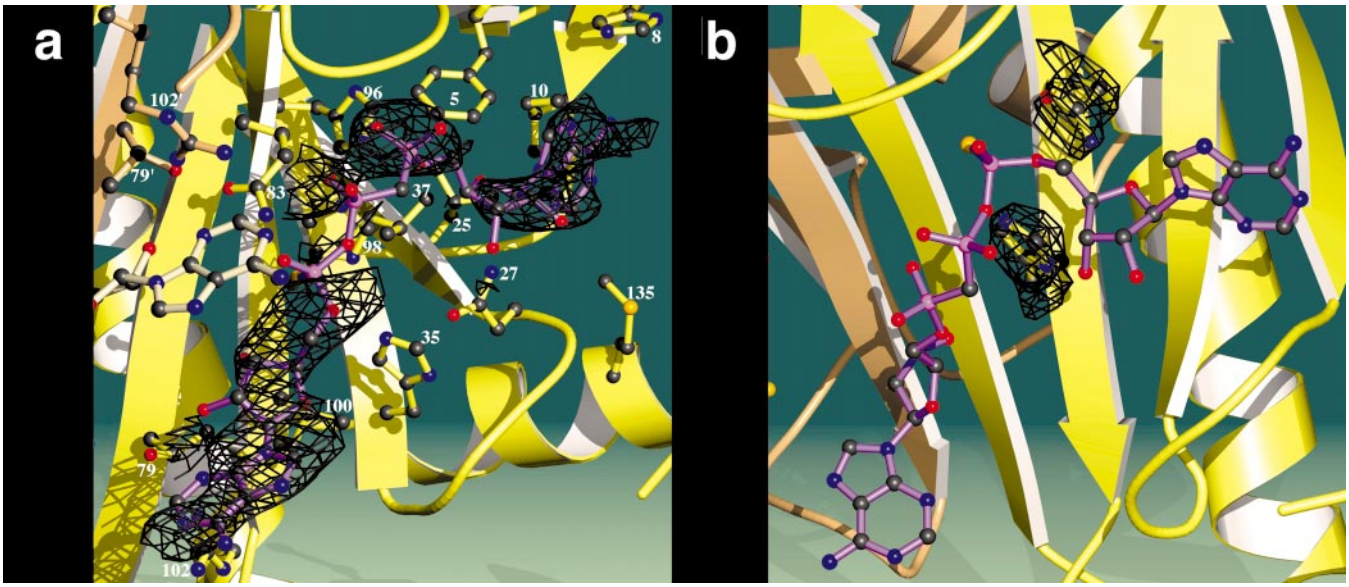

FIG. 3. Conformation and coordination of ApppA analog IB2. (*a*) Difference electron density ($2F_{obs} - F_{calc}$) contoured at 1σ, calculated with IB2 coordinates omitted, superimposed on the refined structure of IB2 in complex with wild-type Fhit. Side chains of coordinating residues are shown. (*b*) Difference electron density ($F_{obs} - F_{calc}$) contoured at 2.0σ, calculated with Asn-96 and His-98 side-chain coordinates omitted, superimposed on the refined structure of IB2 in complex with His96Asn Fhit. Side chains of Asn-96 and His-98 are shown.

The Fhit architecture is formed by a highly curved, 10-stranded antiparallel β-sheet, termed a galactose-1-phosphate uridylyltransferase half-barrel (25), which presents nucleotides on the top surface and buries long helices in the interior (1). The Fhit–IB2 structures, like those of the first Fhit structures, contains an amino-terminal β-hairpin not found in Hint and a gap from residue 107 to residue 127 or to 128 that is disordered (Fig. 2).

For each Fhit-IB2 complex, difference electron density defined a chemically unique and stereospecific mode of IB2 binding per monomer of Fhit (Fig. 3 and Materials and Methods) that ordered several side chains in Fhit for which no role had been described (Fig. 4). When the Fhit polypeptide contained the wild-type His residue at position 96, IB2 (Ado-p-CH_2-p-p_s-Ado) bound with the P^1 phosphate near His-96 and the P^1-P^2 methylene near His-98. Judging from the largest

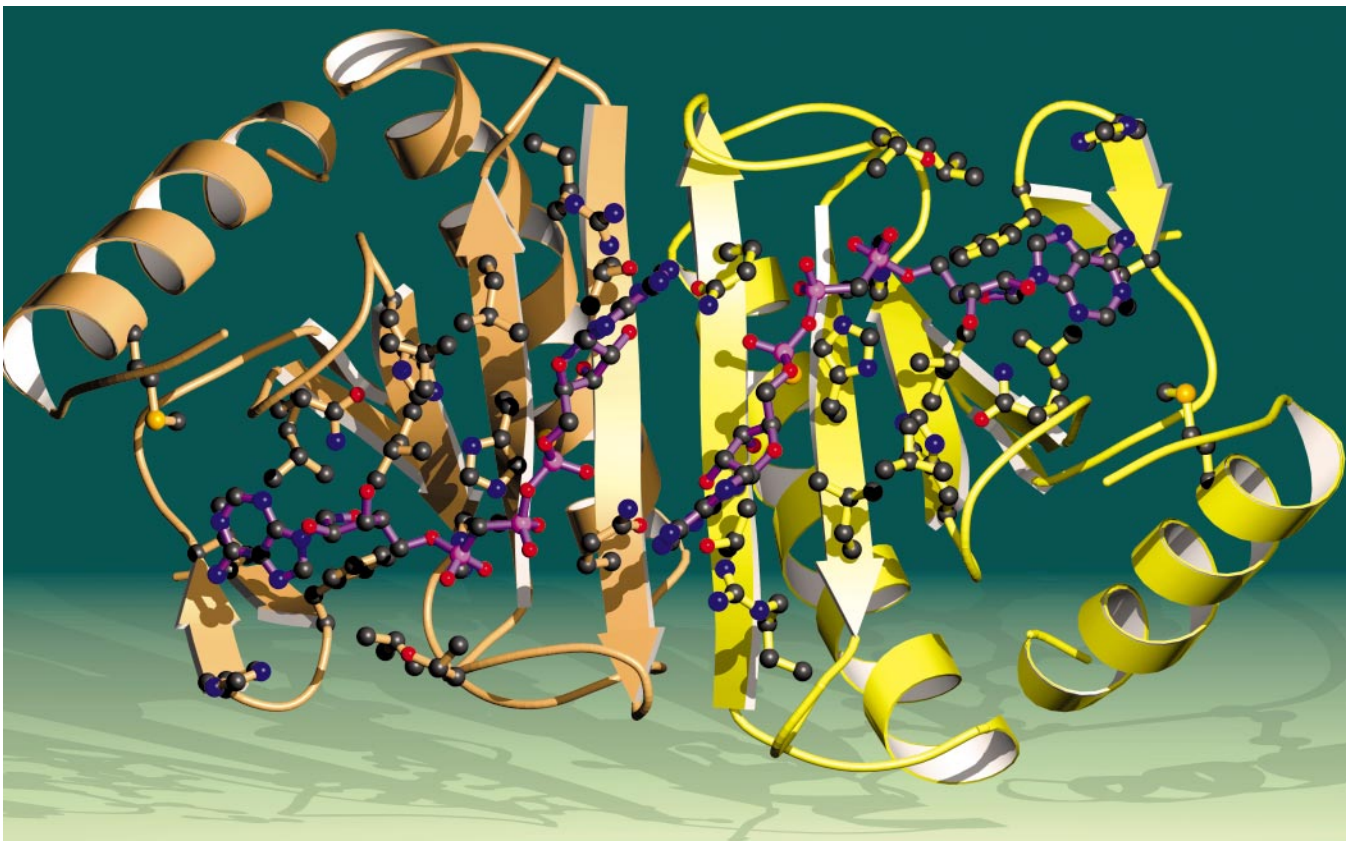

FIG. 4. Top view of the Fhit dimer with two bound IB2 molecules. Two ApppA analog molecules fill a long groove in the top of the wild-type Fhit dimer that is hydrophobic at its (left and right) extremities and lined with polar histidine, glutamine, and arginine residues in its interior.

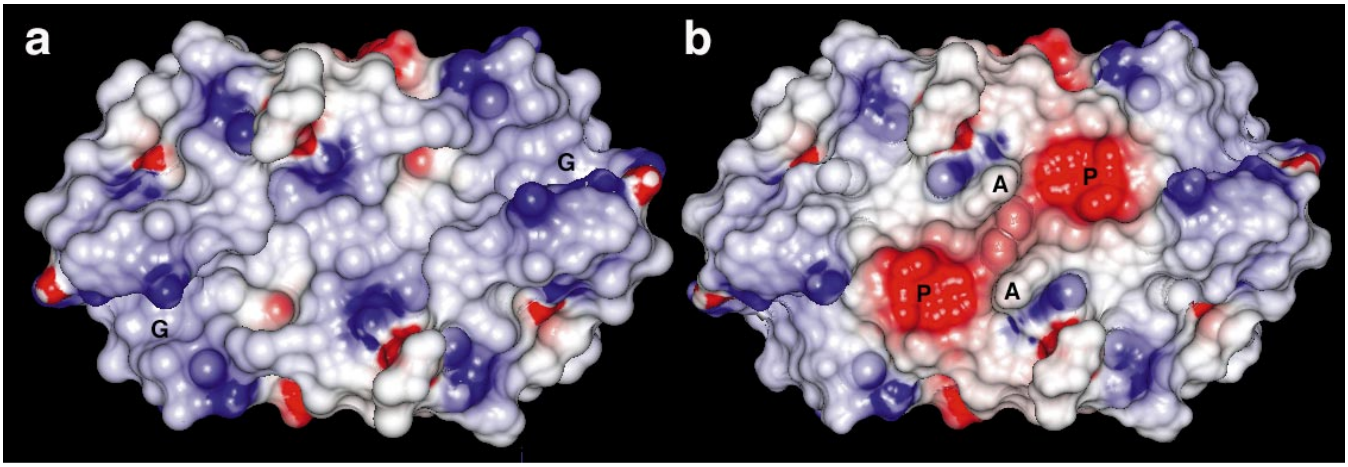

FIG. 5. Electrostatic surface changes mediated by substrate analog binding. (*a*) The electrostatic surface potential of the protein portion of the dimeric wild-type Fhit-IB2 complex, calculated with DELPHI (24), displayed on a scale from bright red (strongly negative) to bright blue (strongly positive). An extensive groove in the Fhit dimer surface runs between the letters G. (*b*) The electrostatic surface potential of the dimeric Fhit-IB2 complex. Two IB2 molecules completely fill the groove. The two bright red blobs marked P are polyphosphate chains. Two surface adenine groups are marked A.

peak of difference electron density, wild-type Fhit selected the *S* stereoisomer of IB2 and buried the sulfur near Leu-100 (Fig. 3*a*). When the Fhit polypeptide contained Asn-96, IB2 bound in the reversed conformation, with the P^3 phosphothio group near Asn-96. In addition to the P^3 for P^1 conformational reversal, difference electron density indicated that His96Asn Fhit selected the *R* stereoisomer (Fig. 3*b*) of the racemic IB2 preparation (17).

Of the six residues in Fhit that create a hydrophobic pocket for the first adenine base, three (Phe-5, Leu-25, and the alkyl chain of Arg-28) are identical or similar to corresponding residues in Hint (1), whereas three side chains are conserved only within the Fhit subfamily. His-8 is always aromatic in the Fhit group, Ile-10 is always Ile or Val, and Met-135 is completely conserved. Interactions with the ribose of the first adenosine are conferred, as in Hint, by His-35, Leu-37, and Val-92. HIT proteins of the Fhit branch contain Asn-27 that aligns with an Asp in Hint homologs. This change may be responsible for decreased repulsive interactions with the 2′ and 3′ oxygens of the ribose. At the P^1 phosphate, His-96 is positioned as is His-112 in Hint. In the complex between His96Asn Fhit and IB2 (Fig. 3*b*), His-98 is positioned to donate a hydrogen bond to the P^2–P^3 bridging oxygen of IB2. A hydrogen bond donated by the backbone amide proton of Gly-13 of Ras to the scissile bridging oxygen of GTP was proposed to be strengthened in the Ras GTPase transition state and thus contribute to catalysis (26). Such a role could account for the ≈300-fold defect in specific activity of the His98Asn mutant form of Fhit (11). Because the wild-type Fhit-IB2 complex contains an electropositive methylene substitution for the scissile group, the complex between His96Asn and IB2 was necessary to see the interaction between His-98 and the bridging oxygen.

The binding site for the second adenosine of ApppA substrates is formed by polar contacts with Thr-79 and Gln-83 and nonpolar interactions with Val-31, Val-32, Leu-100, and Arg-102. Conservation of five of these six residues is diagnostic for the Fhit branch of the HIT protein superfamily, whereas Leu-100 is largely conserved in the entire HIT superfamily (1). Thus, contacts with IB2 paint a surface of functionally important sequence conservation on the Fhit branch of the HIT protein superfamily.

Binding ApppA Analogs Creates a Large Change in Surface Electrostatic Potential and Hydrophobicity. As shown in Fig. 5*a*, the unliganded dimer contains a deep groove which is hydrophobic at its extremes and lined with six histidines, two arginines, and two glutamines in its interior. Upon binding ApppA analogs (Fig. 5*b*), the groove is filled and displays six negatively charged phosphate groups and two adenines on its top surface.

DISCUSSION

Recent results (14) and those presented herein exclude the possibilities that the function of Fhit in tumor suppression depends on ApppA catabolism or signaling by virtue of formation of an enzyme-AMP intermediate and are consistent with a cellular mechanism in which Fhit signals as an enzyme–substrate complex to a putative anti-proliferative or pro-apoptotic effector. The possibility that tumor-suppressor function of Fhit is independent of nucleotide binding is not directly addressed by these experiments. However, the remarkable spatial (Fig. 6) and electrostatic (Fig. 5) complementarity between Fhit and nucleotide substrates and earlier observations on the identities of residues conserved in the HIT superfamily (1) argue that Fhit has been conserved as a nucleotide-binding protein. Nonetheless, this hypothesis must be tested genetically. As can be seen in Fig. 6, substitution of hydrophobic residues forming the first adenine pocket with Trp would be expected to hinder substrate binding. If forma-

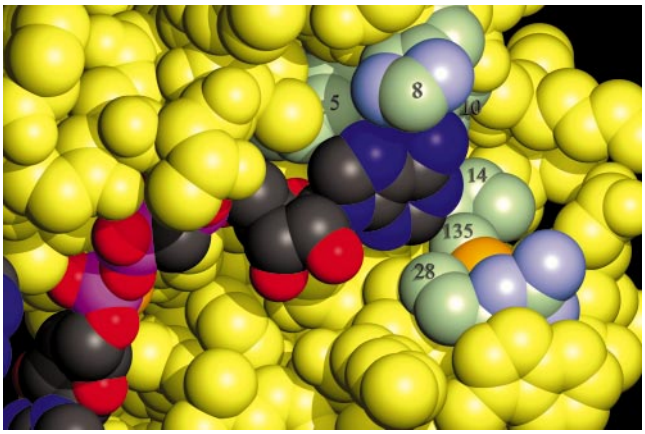

FIG. 6. van der Waals surface of nucleotide-binding site of Fhit. Wild-type Fhit monomer complexed with the ApppA analog IB2 is shown in a space-filling model. Side chains of Phe-5, His-8, Ile-10, Val-14, Leu-25, Arg-28, and Met-135 form a hydrophobic pocket for the adenine base. Bulky substitutions of these residues would be expected to hinder substrate binding.

tion of an enzyme–substrate complex is required for tumor-suppressor function, then these Trp substitution alleles of Fhit would be expected to lose function in parallel with a loss of ability to bind substrates. This loss of function would be expected to be epistatic to the functional but catalytically inactive His96Asn substitution. If, on the contrary, Trp substitution alleles bind substrates poorly but are phenotypically wild type, strong evidence would be provided for a nucleotide-independent mechanism.

The substrate-dependent mechanism proposed for Fhit protein function shares some features with G-protein regulation and some features with proteins regulated by phosphorylation. G proteins such as Ras and Gα have altered protein–protein interactions in their GTP and GDP forms that are mediated in part by protein conformational changes. While we have argued that Fhit is likely to signal in substrate-bound forms, the protein portion of the Fhit–substrate complex is not significantly changed by substrate binding. Relative to a proposed ground state of Fhit that might be nucleotide-free or associated with AMP products, Fhit–ApppA complexes or Fhit-diadenosine tetraphosphate complexes would display four to eight additional surface phosphates and two surface adenosines. Judging from the kinetics presented in Table 1, this modification of the Fhit protein surface is likely to be transient and exquisitely sensitive to the concentrations of Fhit substrates. Cellular conditions that produce Fhit substrates would act like a protein kinase, resulting in deposition of phosphates (and adenosines) on the Fhit surface. The intrinsic hydrolytic activity of Fhit would act like a protein phosphatase, releasing the modification. As we have argued earlier, substrates that associate well but are turned over slowly would be expected to sustain signaling longer than the "best substrates" (1). A putative Fhit effector that binds Fhit–substrate complexes may actually stabilize such complexes and act as an inhibitor of the Fhit reaction.

We thank Christopher D. Lima of Columbia University for coordinates of unliganded Fhit protein. This work was supported by grants from the National Cancer Institute, R01CA75954 (C.B.), P30CA56036, P01CA21124, T32CA09662, and T32CA09678; the National Science Foundation, MCB-9604124 (L.D.B.); and the Biotechnology and Biological Sciences Research Council, CHM.RA73559. 2514 (G.M.B.). CHESS is supported by the National Science Foundation (DMR-9311772) and the National Institutes of Health (RR-01646). C.B. is a Basil O'Connor Scholar of the March of Dimes Birth Defects Foundation, a Beckman Young Investigator of the Arnold and Mabel Beckman Foundation, and a Burroughs Wellcome Foundation New Investigator in the Basic Pharmacological Sciences.

1. Brenner, C., Garrison, P., Gilmour, J., Peisach, D., Ringe, D., Petsko, G. A. & Lowenstein, J. M. (1997) *Nat. Struct. Biol.* **4,** 231–238.
2. Ohta, M., Inoue, H., Cotticelli, M. G., Kastury, K., Baffa, R., Palazzo, J., Siprashvili, Z., Mori, M., McCue, P., Druck, T., Croce, C. M. & Huebner, K. (1996) *Cell* **84,** 587–597.
3. Mao, L., Lee, J. S., Kurie, J. M., Fan, Y. H., Lippman, S. M., Lee, J. J., Ro, J. Y., Broxson, A., Yu, R., Morice, R. C., Kemp, B. L., Khuri, F. R., Walsh, G. L., Hittelman, W. N. & Hong, W. K. (1997) *J. Natl. Cancer Inst.* **89,** 857–862.
4. Sozzi, G., Veronese, M. L., Negrini, M., Baffa, R., Cotticelli, M. G., Inoue, H., Tornielli, S., Pilotti, S., De Gregorio, L., Pastorini, U., Pierotti, M. A., Ohta, M., Huebner, K. & Croce, C. M. (1996) *Cell* **85,** 17–26.
5. Negrini, M., Monaco, C., Vorechovsky, I., Ohta, M., Druck, T., Baffa, R., Huebner, K. & Croce, C. M. (1996) *Cancer Res.* **56,** 3173–3179.
6. Virgilio, L., Schuster, M., Gollin, S. M., Veronese, M. L., Ohta, M., Huebner, K. & Croce, C. M. (1996) *Proc. Natl. Acad. Sci. USA* **93,** 9770–9775.
7. Druck, T., Hadaczek, P., Fu, T. B., Ohta, M., Siprashvili, Z., Baffa, R., Negrini, M., Kastury, K., Veronese, M. L., Rosen, D., Rothstein, J., McCue, P., Cotticelli, M. G., Inoue, H., Croce, C. M. & Huebner, K. (1997) *Cancer Res.* **57,** 504–512.
8. Sozzi, G., Sard, L., De Gregorio, L., Marchetti, A., Musso, K., Buttitta, F., Tornielli, S., Pellegrini, S., Veronese, M. L., Manenti, G., Incarbone, M., Chella, A., Angeletti, C. A., Pastorino, U., Huebner, K., Bevilaqua, G., Pilotti, S., Croce, C. M. & Pierotti, M. A. (1997) *Cancer Res.* **57,** 2121–2123.
9. Greenspan, D. L., Connolly, D. C., Wu, R., Lei, R. Y., Vogelstein, J. T. C., Kim, Y. T., Mok, J. E., Munoz, N., Bosch, F. X., Shah, K. & Cho, K. R. (1997) *Cancer Res.* **57,** 4692–4698.
10. Sozzi, G., Tornielli, S., Tagliabue, E., Sard, L., Pezzella, F., Pastorini, U., Minoletti, F., Pilotti, S., Radcliffe, C., Veronese, M. L., Goldstraw, P., Huebner, K., Croce, C. M. & Pierotti, M. A. (1997) *Cancer Res.* **57,** 5207–5212.
11. Barnes, L. D., Garrison, P. N., Siprashvili, Z., Guranowski, A., Robinson, A. K., Ingram, S. W., Croce, C. M., Ohta, M. & Huebner, K. (1996) *Biochemistry* **35,** 11529–11535.
12. Zimonjic, D. B., Druck, T., Ohta, M., Kastury, K., Croce, C. M., Popescu, N. C. & Huebner, K. (1997) *Cancer Res.* **57,** 1166–1170.
13. Boldog, F., Gemmill, R. M., West, J., Robinson, M., Robinson, L., Li, E. F., Roche, J., Todd, S., Waggoner, B., Lundstrom, R., Jacobson, J., Mullokandov, M. R., Klinger, H. & Drabkin, H. A. (1997) *Hum. Mol. Genet.* **6,** 193–203.
14. Siprashvili, Z., Sozzi, G., Barnes, L. D., McCue, P., Robinson, A. K., Eryomin, V., Sard, L., Tagliabue, E., Greco, A., Fusetti, L., Schwartz, G., Pierotti, M. A., Croce, C. M. & Huebner, K. (1997) *Proc. Natl. Acad. Sci. USA* **94,** 13771–13776.
15. Brenner, C., Pace, H. C., Garrison, P. N., Robinson, A. K., Rösler, A., Liu, X., Blackburn, G. M., Croce, C. M., Huebner, K. & Barnes, L. D. (1997) *Protein Eng.* **10,** 1461–1463.
16. Lima, C. D., Damico, K. L., Naday, I., Rosenbaum, G., Westbrook, E. M. & Hendrickson, W. A. (1997) *Structure* **5,** 763–774.
17. Blackburn, G. M., Liu, X., Rösler, A. & Brenner, C. (1998) *Nucleosides Nucleotides* **17,** 301–308.
18. Lima, C. D., Klein, M. G. & Hendrickson, W. A. (1997) *Science* **278,** 286–290.
19. Collaborative Computing Project, Number 4 (1994) *Acta Crystallogr. D* **50,** 760–763.
20. Barnes, L. D., Robinson, A. K., Mumford, C. H. & Garrison, P. N. (1985) *Anal. Biochem.* **144,** 296–304.
21. Brünger, A. T. (1997) *Methods Enzymol.* **277,** 366–396.
22. Jones, T. A., Zou, J. Y., Cowan, S. W. & Kjeldgaard, M. (1991) *Acta Crystallogr. A* **47,** 110–119.
23. Kraulis, P. J. (1991) *J. Appl. Crystallogr.* **24,** 946–950.
24. Nicholls, A. & Honig, B. (1991) *J. Comput. Chem.* **12,** 435–445.
25. Wedekind, J. E., Frey, P. A. & Rayment, I. (1995) *Biochemistry* **34,** 11049–11061.
26. Maegley, K. A., Admiraal, S. J. & Herschlag, D. (1996) *Proc. Natl. Acad. Sci. USA* **93,** 8160–8166.